RSC Advances

ROYAL SOCIETY OF CHEMISTRY

www.rsc.org/advances

Journal Name

RSCPublishing

COMMUNICATION

In-situ solution plasma synthesis of mesoporous nanocarbon-supported bimetallic nanoparticles

Cite this: DOI: 10.1039/x0xx00000x

Jun Kang[a*], Nagahiro Saito[b]

Received ooth January 2012,
Accepted ooth January 2012

DOI: 10.1039/x0xx00000x

www.rsc.org/

Herein, it is reported that a novel *in-situ* one-step synthesis method of bimetallic nanoparticles (NPs) supported on carbon blacks, which can markedly prevent the aggregation and growth of NPs, resulting in a small particle size (average 5 nm), good dispersion, and high-electrocatalytic-activity.

Recently, bimetallic nanoparticles (NPs), composed of two different metallic elements, have received considerable attention for their unique optical, magnetic, and catalytic properties.[1–5] They are particularly important in the field of electrocatalysis since they often exhibit better catalytic properties than their monometallic counterparts owing to strong synergy between the metals. For example, the low durability of Pt catalyst in the cathode of fuel cells can be improved to some extent by the addition of another metal.[6-10] In addition, Au catalyst promotes the discharge process (oxygen reduction reaction, ORR), and Pt catalyst promotes the charge process (oxygen evolution reaction, OER) in a Lithium−air (Li−air) battery.[11] For this reason, AuPt bimetallic NPs have been shown to strongly enhance the kinetics of the ORR and OER in rechargeable $Li–O_2$ cells, and its cells exhibit the highest round-trip efficiency reported to date.[12] Hence, the mixing of metals is a way of developing new materials that have higher technological usefulness than their starting substances.

Meanwhile, synthesizing bimetallic NPs while maintaining small particle size is too difficult because the formation of intermetallic phases generally requires high temperatures, which easily leads to the aggregation NPs.[13] By applying chemical reduction methods, bimetallic nanoparticles can be prepared at low temperature, but it is generally necessary to use a large amount of stabilizer or surfactant, which causes catalytic activity degradation.

In addition, to obtain novel properties and efficiency of the catalyst, the uniformity of NP dispersion on the supporting material is required. However, to date, reported composites containing highly-dispersed NPs in carbon supports are based on rather complicated synthetic procedures, i.e., fabricating porous carbon support materials, introducing a metal salt on the porous carbon, and then reducing the metal salt to metal with hydrogen gas or by electrodeposition.[14–17] These procedures require considerable metal salt and involve a multi-step fabrication process that frequently results in aggregated metal particles, which, in turn, lowers the available surface area and decreases the mass activity of catalyst.

In this work, we report a new simple synthesis method for generating nanocarbon-supported bimetallic NPs. Au-Pt bimetallic NPs were synthesized simultaneously with carbon black by innovative method, the Solution Plasma Process (SPP). Previous studies have shown the ability of this process to successfully synthesize nanoparticles, including nanocolloidal particles, metal nanoparticles, and carbon-related materials by SPP.[18–25] The purpose of this study was to apply the progressive solution plasma process in the field of bimetallic NPs/C synthesis and to simplify the multiple processes.

The experimental setup for bimetallic NPs/C by an SPP is shown in Fig. 1a. Experiments were carried out at room temperature and atmospheric pressure conditions. The gold and platinum wires served as opposite electrodes at the corresponding NPs precursors, and each electrode was covered with a ceramic tube that was inserted in a silicone stopper. The electrodes were then placed in a 100mL glass beaker having an inner diameter of 50 mm and a height of 70 mm. The distance between the tips of electrodes was set to 0.5 mm. Before the discharge, the glass beaker was filled with benzene (C_6H_6) solution, serving as the basic carbon precursor. A bipolar pulsed power generator was applied to generate the discharge. The pulse width and frequency of the power supply were fixed at 0.5 μs and 25 kHz, respectively. After the discharge process, the obtained solution was filtered and the residual carbon particles were dried in a oven at 80°C. Then the solution was heat-treated at 700°C for 30 minutes under an argon atmosphere. Heat treatment was required to increase the conductivity of the carbon matrix. The detailed information of synthetic procedure and characterization is given in ESI†.

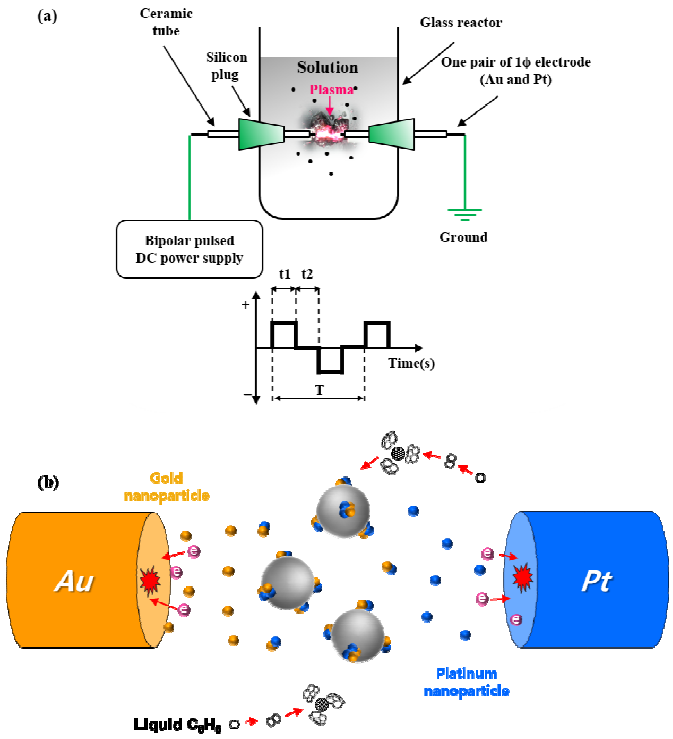

Fig. 1 Schematic of the solution plasma process (SPP) and formation mechanism of AuPt bimetallic NPs/C.

Fig. 1b shows the fabrication model of AuPt bimetallic NPs/C by SPP. The solution plasma provides a novel reaction field with a highly energetic state for the formation of carbon-supported AuPt bimetallic NPs. From the plasma region, various radicals such as C, C_2, CH, and Hα were generated.[22] Along with the bombardment of highly energetic radical particles and electrons, numerous metal atoms were generated from the electrode surfaces under sputtering because the electrodes were continuously bombarded by energetic radicals and electrons. These atoms formed small bimetallic particles, and they were loaded onto the simultaneously synthesized carbon blacks.

Fig. 2 shows a field emission scanning electron microscopy (FESEM) image, bright field scanning images, transmission electron microscopy (BF-STEM) images, and energy dispersive X-ray analysis (EDX) analysis of as-prepared AuPt bimetallic NPs/C. The NPs exist stably without any aggregation or impurities, giving clean clusters that were ideal for catalytic studies. These images (Figs. 2b and c) clearly revealed that the spherical AuPt NPs were remarkably uniform and homogenous. Owing to the nearly simultaneous formation of AuPt NPs and carbon black particles occurring during plasma sputtering, well-crystallized bimetallic NPs (SAED pattern and HR-TEM image shows in Fig. S1 ESI†) were equably distributed over the entire surface of the carbon blacks. The image (Fig. S2 ESI†) showed that the AuPt bimetallic NPs had a narrow size distribution with an average size of 4–5 nm. The average particle size of NPs was also calculated based on the broad peak areas from the X-Ray Diffraction (XRD) pattern using Scherrer's formula and it was 5.5nm.[26] This result agreed with the TEM observations. The distribution of Au and Pt elements in the clusters was investigated by EDX attached to STEM. The Au Lα & Mα emission and Pt Lα & Mα emission were detected plainly for each isolated particle (Figs. 2 d and e). EDX analysis indicated that every NP contained both Au and Pt elements. These results clarified that each particle is an AuPt bimetallic NP. It should be noted that these measurements limit the degree of accuracy because of the small size of the clusters (large magnification) and sample drifting during the measurement. Based on the EDX spectrums, the average atomic ratio between Pt and Au was 44 : 56 (Fig. S4 ESI†).

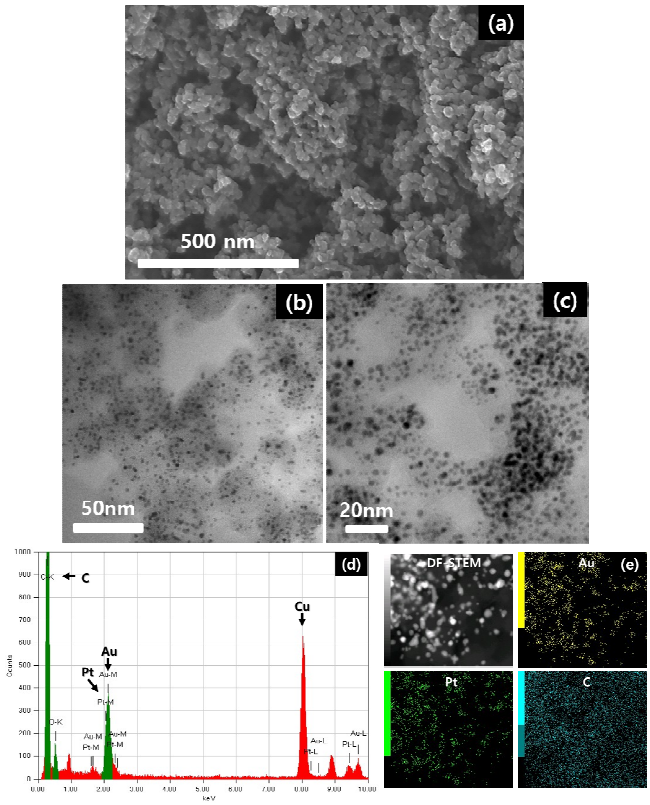

Fig. 2 (a) FESEM image and (b and c) STEM image of AuPt bimetallic NPs/C (d and e) EDS spectrum and mapping of AuPt bimetallic NPs/C

XRD analysis was carried out on powder samples to compare the diffraction pattern of bimetallic AuPt NPs with that of standard JCPDS cards of Au and Pt(Au-JCPDS No 65-2870), Pt-JCPDS No 62-2868), as shown in Fig. 3. The two broad peaks located between (111) peak of Pt (2θ = 39.755°) and Au (2θ = 38.188°), and (200) peak of Pt (2θ = 46.236°) and Au (2θ = 44.386°), respectively.

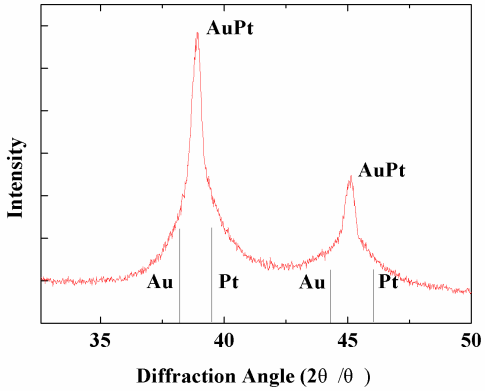

Fig. 3 X-ray diffraction patterns for AuPt bimetallic NPs/C.

The fact that the peaks of (111) and (200) lie between those of monometallic Au and Pt supports the formation of bimetallic AuPt NPs. The sharp peaks were attributed to abnormally large NPs, which were observed very rarely in the TEM images. Based on the calculations from the peak area, the size of these particles was in the range of approximately 20 to 30 nm, and it is believed that these large particles were occasionally generated by locally concentrated sputtering on the surface electrode. It is believed that these results illustrate the formation of AuPt bimetallic NPs.

In order to investigate the electrochemical activity of carbon-supported AuPt bimetallic NPs, cyclic voltammetry were carried out in N_2-saturated 1 M H_2SO_4 solution. A comparison of the cyclic voltammograms is shown in Fig. 4. The shapes of the cyclic voltammograms for monometallic Pt and Au NPs/C electrodes synthesized by SPP are shown in the images. The shape of the cyclic voltammogram of Au–Pt has the characteristics of both metals. The cyclic voltammogram of as-prepared samples shown in Fig. S4 ESI†. In the cathodic direction, in the potential region of $0.8 < E < 1.1$ V, reduction of Au oxide was observed followed by the reduction of Pt oxide. The adsorption and deposition of hydrogen occurred between 0.05 and 0.2 V. Furthermore, the results showed a sharp and clear cathodic current. These characteristics were very similar to those of a monometallic NPs/C electrode. This indicated the high electrocatalytic activity of the carbon-supported AuPt bimetallic NPs in the oxygen reduction reaction (ORR) and hydrogen evolution reaction (HER), which is an important factor for catalytic reactions. Thus, this cyclic voltammogram result clarified good ORR and HER activity of AuPt catalyst. This work shows that placing select atoms (such as transition metal) on nanoparticle can be a promising strategy to develop new highly active catalysts.

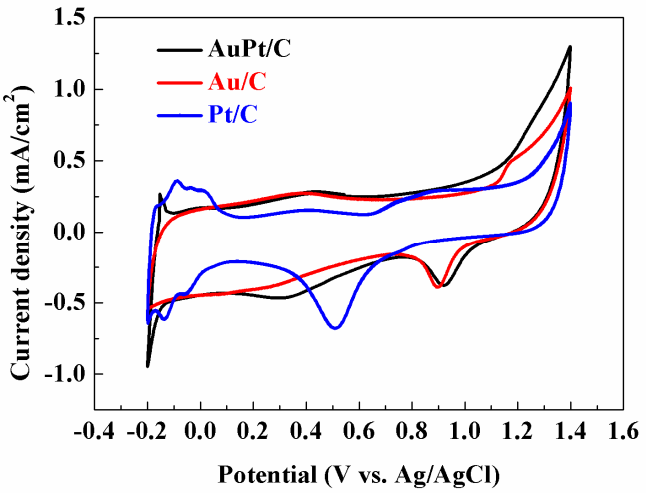

Fig. 4 Cyclic voltammetry plots for AuPt/C and their corresponding monometallic NPs/C electrode.

Other structural specifications including the total surface area, total pore volume, and mean pore diameter of the AuPt bimetallic NPs/C were determined using the Brunauer Emmett Teller (BET) method. The details of the N_2 adsorption–desorption isotherms and structural parameters of AuPt bimetallic NPs/C are shown in Fig. S5 ESI† and are summarized in Table S1 (ESI†). The isotherms exhibited type-IV and H1-type hysteresis loop characteristics according to the IUPAC classification.[27–29] The total surface area, total pore volume, and mean pore size were in the range of 331 (m^2g^{-1}) and 1.42 (cm^3g^{-1}), 14.6 (nm), respectively. From these results, it is assumed that synthesized carbon-black presented highly mesoporous structures, and this structure promotes the diffusion of chemical species into the inner parts of the carbon, leading to the active use of the catalyst on its surface.

Conclusions

Noble bimetallic NPs were successfully synthesized simultaneously with carbon black via a solution plasma process. The gold and platinum wires served as opposite electrodes for the corresponding NP precursors, and benzene solution served as the carbon precursor. As-obtained AuPt bimetallic NPs were confirmed to be alloy by the XRD, TEM and EDX of each particle. Cyclic voltammograms clarified that AuPt bimetallic NPs nanoclusters have a good electrocatalytic property corresponding to the obvious oxidation and reduction features. This work shows that a combination of various kinds of electrode material can be a promising strategy to develop highly active electrode materials. This method is a potential candidate for the next-generation one-step synthesis of bimetallic NPs/carbon.

Acknowledgement

This study was supported by 2014 Korea Maritime & Ocean University research grant for new faculty.

Notes and references

[a] Korea Maritime and Ocean University, Yeongdo-Gu, Busan, Korea
[b] Nagoya University, Furo-cho, Chikusa-ku, Nagoya, Japan

1. N. Toshima and T. Yonezawa, *New J. Chem.*, 1998, **22**, 1179
2. A. V. Di Wang, F. Porta, L. Prati and D. Su, *J. Phys. Chem. C*, 2008, **112**, 8617.
3. Y. W. Lee, M. J. Kim, Z. H. Kim and S. W. Han, *J. Am. Chem. Soc.*, 2009, **131**, 17036.
4. C. H. Chen, L. S. Sarma, J. M. Chen, S. C. Shih, G. R. Wang, D. G. Liu, M. T. Tang, J. F. Lee and B. J. Hwang, *ACS Nano*, 2007, **1**, 114.
5. N. Chandrasekhar and D. S. Sholl, *J. Alloy. Compd.*, 2014, **609**, 244.
6. T. J. Schmidt, H. A. Gasteiger and R. J. Behm, *Langmuir*, 1997, **13**, 2591.
7. Q. Yuan, Z. Zhou, J. Zhuang and X. Wang, *Chem. Comm.*, 2010, **46**, 1491.
8. Y. Y. Tong, H. S. Kim, P. K. Babu, P. Waszczuk, A. Wieckowski and E. Oldfield, *J. Am. Chem. Soc.*, 2002, **124**, 468
9. M. Arenz, V. Stamenkovic, B. Blizanac, K. Mayrhofer, N. Markovic and P. Ross, *J. Catal.*, 2005, **232**, 402.
10. G. T. Fu, R. G. Ma, X. Q. Gao, Y. Chen, Y. W. Tang, T. H. Lu and J. M. Lee, *Nanoscale*, 2014, **6**, 12310
11. Y. C. Lu, H. A. Gasteiger, E. Crumlin, R. McGuire and Y. Shao-Horn, *J. Electrochem. Soc.*, 2010, **157**, A1016.
12. Y. C. Lu, H. A. Gasteiger, S. Chen, H. S. Kimberly and S. H. Yang, *J. Am. Chem. Soc.*, 2010, **132**, 12170.
13. S. Takenaka, A. Hirata, E. Tanabe, H. Matsune and M. Kishida, *J. Catal.*, 2010, **274**, 228.
14. S. H. Joo, I. Oh, J. Kwak, Z. Liu, O. Terasaki and R. Ryoo, *Nature*, 2001, **412**, 169
15. V. K. B. Rajesha, S. Karthikeyana, K. R. Thampib, and B. V. J.-M. Bonardc, *Fuel*, 2002, **81**, 2177.
16. C. Wang, M. Waje, X. Wang, J. M. Tang, R. C. Haddon and Y. Yan, *Nano Lett.*, 2004, **4**, 345.

17. H. Tang, J. H. Chen, Z. P. Huang, D. Z. Wang, Z. F. Ren, L. H. Nie, Y. F. Kuang and S. Z. Yao, *Carbon*, 2004, **42**, 191.
18. N. Saito, J. Hieda and O. Takai, *Thin Solid Films*, 2009, **518**, 912.
19. M. A. Bratescu, N. Saito and O. Takai, *Curr. Appl. Phys.*, 2011, **11**, 1.
20. J. Kang, O. L. Li and N. Saito, *Carbon*, 2013, **60**, 292.
21. J. Kang, O. L. Li and N. Saito, *J. Power Sources*, 2014, **261**, 156.
22. J. Kang, O. L. Li and N. Saito, *Nanoscale*, 2013, **5**, 6874.
23. D. W. Kim, O. L. Li and N. Saito, *Phys Chem Chem Phys.*, 2014, **16**, 14905.
24. D. W. Kim, O. L. Li and N. Saito, *Phys Chem Chem Phys.*, 2015, **17**, 407.
25. G. Panomsuwan, S. Chiba, Y. Kaneko, N. Saito and T. Ishizaki, *J. Mater. Chem. A*, 2014, **2**, 18677.
26 L. V. Azaroff, Elements of X-Ray Crystallography, McGraw-Hill, NewYork, USA, 1968, p. 549.
27 J. Rouquerol, D. Avnir, C. W. Fairbridge, D. H. Everett, J. M. Haynes, N. Pernicone, J. D. F. Ramsay, K. S. W. Sing and K. K. Unger, *Pure Appl. Chem.*, 1994, **66**, 1739.
28 H. M. Kao, T. Y. Shen, J. D. Wu and L. P. Lee, *Microporous Mesoporous Mater.*, 2008, **110**, 461.
29 Y. Wang, S. Zhu, Y. Mai, Y. Zhou, X. Zhu and D. Yan, *Microporous Mesoporous Mater.*, 2008, **114**, 222.

